IEEE Access
Multidisciplinary ⋮ Rapid Review ⋮ Open Access Journal

Received 25 July 2024, accepted 20 August 2024, date of publication 29 August 2024, date of current version 10 September 2024.

Digital Object Identifier 10.1109/ACCESS.2024.3451956

RESEARCH ARTICLE

Low-Cost, Point-of-Care Potassium Ion Sensing Electrode in EGFET Configuration for Ultra-High Sensitivity

VISHNURAM ABHINAV[1], (Graduate Student Member, IEEE), AND TEJAS R. NAIK[1,2]
[1]Indian Institute of Technology Bombay, Mumbai 400076, India
[2]University of Glasgow, G12 8QQ Glasgow, U.K.

Corresponding author: Vishnuram Abhinav (vishnuram.abhinav@gmail.com)

ABSTRACT This paper presents the development of a non-toxic and low-cost potassium ion sensor utilizing an Extended Gate Field-Effect Transistor (EGFET) configuration with all-solid-state electrodes fabricated on a printed circuit board (PCB) substrate. An Ag/AgCl-based pseudo-reference electrode (PRE) has been fabricated planar to a ion-selective membrane (ISM) coated on the gold solid-contact electrode (SCE). The PRE has shown $< 1\ mV/day$ drift potential, exhibiting exceptional stability and reproducibility. While the SCE has demonstrated a high sensitivity of 49 $mV/log[K^+]$, covering a wide linear detection range from $10^{-4}\ M$ to $1\ M$ with a rapid response time of less than 10 seconds. The sensor has displayed minimal hysteresis ($< 15\ mV$) and remained stable over a broad pH range (pH 4 to pH 10). These uni-planar, all-solid-state electrodes along with off-the-shelf FET mitigate the requirement of additional wire bonding by utilizing a common PCB platform for sensing as well as circuitry area. Additionally, the PRE, SCE and the FET in the EGFET-configuration-based sensing system have exhibited a high current sensitivity of 1.43 $(\mu A)^{1/2}/log[K^+]$. Our sensor presents a practical and reliable solution for soil nutrient measurement in precision agriculture, offering significant advantages over existing potassium sensors in terms of cost-effectiveness, sensitivity, stability, and environmental safety. The presented approach holds promise for optimizing agricultural productivity and minimizing environmental impact through efficient nutrient monitoring and smart irrigation and fertilization management systems.

INDEX TERMS EGFET, solid-contact electrode, ion-sensor, potentiometry, crown-ether.

I. INTRODUCTION

The agricultural industry, on a global scale, has incurred substantial losses, totalling an estimated $ 3.8 trillion in production value [1]. These losses, averaging $ 123 billion annually, are attributed to multifaceted factors including nutrient mismanagement. To effectively address this challenge, the agricultural sector requires advanced sensor technologies capable of providing accurate and real-time data on soil nutrient concentrations. Specifically, the development of ion sensors for soil nutrient monitoring is essential for optimizing agricultural practices, minimizing losses, and enhancing the overall productivity in a sustainable manner.

Potassium is one of the significant nutrients (NPK) for crop growth and development. Consequently, detecting the potassium ion (K^+) in the soil is a critical element of agriculture. Traditional methods for soil analysis have involved collecting field samples and examining them in a laboratory. Techniques such as near-infrared (NIR) spectroscopy and X-ray fluorescence (XRF) have been employed to measure components like potassium ions (K^+) [2], [3]. These lab-based methods have provided precise data on soil composition and nutrient levels. However, the current demand for intelligent irrigation and fertilization management has led to the design of instruments that can directly obtain information in the field without extensive laboratory work. Thus, other approaches include portable hand-held meters that use conductivity or colorimetry,

The associate editor coordinating the review of this manuscript and approving it for publication was Lei Wang.

as well as ion-selective electrodes (ISEs), which measure the electrical potential (potentiometric measurement) generated by the K^+ ions [4].

Since the 2000s, several studies have highlighted the potential of potentiometric sensors in precision agriculture. Solid-contact electrodes (SCEs) and coated wire electrodes (CWEs) have become more favoured than barrel-type ISEs because they do not require a conventional internal electrolyte inside the electrode structure [5]. The majority of these researchers have developed portable ion-selective electrodes (ISE) or ion-sensitive field-effect transistor (ISFET)-based nutrient measurements in soil extracts [6], [7]. Semiconductor-based ISE or ISFET sensors have been investigated due to the miniaturization and mass production advantages of innovative transducer materials and complementary metal-oxide semiconductor (CMOS) processes [8]. In 2001, Artigas et al. analysed the soil using fabricated pH-ISFET, pK-ISFET, pCa-ISFET, and pNO_3-ISFET sensors [9]. The gate insulator of the ISFET was functionalized with a polymeric ion-selective membrane (ISM) to selectively detect target ions. These devices have problems with polymeric ISM adhering to gate materials such as Al_2O_3 or Si_3N_4 [10]. Often, the target ion diffuses into the oxide or channel of the FET, leading to the degradation of the performance and characteristics of the ISFET. Drifts in FET threshold voltage and packaging issues result from the contact of the electrolyte with the transistor gate region [11]. Hence, isolation of the target ion from the FET device is necessary. Van der Spiegel invented the Extended Gate FET (EGFET) in 1983 as a credible alternative to the ISFET [12]. EGFET has a configuration comparable to that of an ISFET, although its sensing membrane is distant from the FET device, averting chemical interaction. The external gate electrode of the detector is submerged in an electrolytic solution. This chemically changes the FET's threshold voltage [13]. EGFET has replaced ISFET to improve reliability, threshold voltage drift, stability, sensitivity to environmental factors and fast response. Various fabrication techniques have improved packaging, device encapsulation, and production cost efficiency [14], [15].

Commercially available printed circuit board (PCB) technology has provided an easy, efficient, and economical solution for electrode fabrication. This approach has leveraged economies of scale, significantly reducing costs through large-volume manufacturing for the development of various sensors. Bozkurt and Lal designed a PCB microelectrode array for implantable neuromuscular stimulation [16]. Studies on potentiometric sensor development using PCB electrodes have been conducted by Prodromakis et al. [17], Trantidou et al. [18], and Moschou et al. [19]. Prodromakis et al. achieved a $\sim$22 mV/pH sensitivity by sputtering a 150 nm TiO_2 layer on 500 μm Au-plated Cu electrodes, placed on rigid PCB substrates. Trantidou et al. used the same PCB electrode structure, but selectively plasma-treated the Parylene C film deposited on the PCB to achieve a sensitivity of -16.3 mV/pH but a high drift rate of 2.5 - 20 mV/h. Moschou et al. reported rigid PCB-based Ag/AgCl reference electrodes (RE) with 300 μm to 1 mm vias and achieved a low potential drift under 1 mV/20 days at pH 7. A sensitivity of -45.8 mV/pH has been reported using a PCB-based pH sensor with a 200 nm-thick indium tin oxide (ITO) layer. Multi-parametric (H^+, Na^+, and K^+) potentiometric sensing on both ENIG and Hard Gold finish PCB platforms was also demonstrated by Salzitsa Anastasova et al., [20]. In addition to cost, the ENIG and Hard Gold coatings exhibited different sensitivity levels to potassium ions. Although the expensive hard gold displayed a sensitivity of 54 mV/log [K+], the economic ENIG platform exhibited 22.2 mV/log[K+]. Most studies tend to prioritize either cost-effective solutions with compromised sensitivity or highly sensitive approaches at higher costs. Future research should aim to strike a balance between affordability and sensitivity to address this challenge effectively.

Furthermore, the realization of ISEs, valinomycin is a prominent ionophore because of its superior selectivity for potassium ions and sensitivity among all the ionophores [20], [21], [22], [23], [24]. However, the negative effect of valinomycin has been first highlighted by Daniele et al. They have demonstrated that valinomycin inhibits phytohemagglutinin-stimulated blastogenesis and proliferation in human lymphocytes [25]. Apoptosis in certain mammalian cell lines, inhibition of sperm motility [26], collapse of mitochondrial membrane potential [27], neurotoxicity [28], and, among other detrimental effects of valinomycin, have been reported. Valinomycin can be absorbed through the skin, cause irritation, and can also have negative effects when inhaled [29]. Thus, the practical application of valinomycin is inhibited, especially if it is intended for use by non-experts. Non-toxic alternatives to valinomycin are mutacin and crown ether. Crown ether appears to be a promising alternative to valinomycin for SCE because of its suitability for the required sensing range (soil potassium ion range), ease of synthesis, and potential for sensitivity maximization [30].

Several EGFET-based potassium sensing platforms rely on commercial electrodes for measurement, as documented in the literature [31], [32]. However, this reliance presents a significant challenge in terms of portability. To address this issue, stable integrated reference electrodes are required to obtain sensitive and reliable sensor readings in portable devices. Li et al., 2017 have fabricated an Ag/AgCl PRE on a flexible PEN substrate and used it in conjunction with a pH-sensitive ISFET [33]. Similarly, Moschou et al. have fabricated Ag/AgCl PRE on a PCB substrate in combination with pH-selective EGFET, demonstrating excellent long-term stability compared to commercial Ag/AgCl reference electrodes [19].

To address the challenges outlined above, we have presented a low-cost, fast and non-toxic sensor for soil

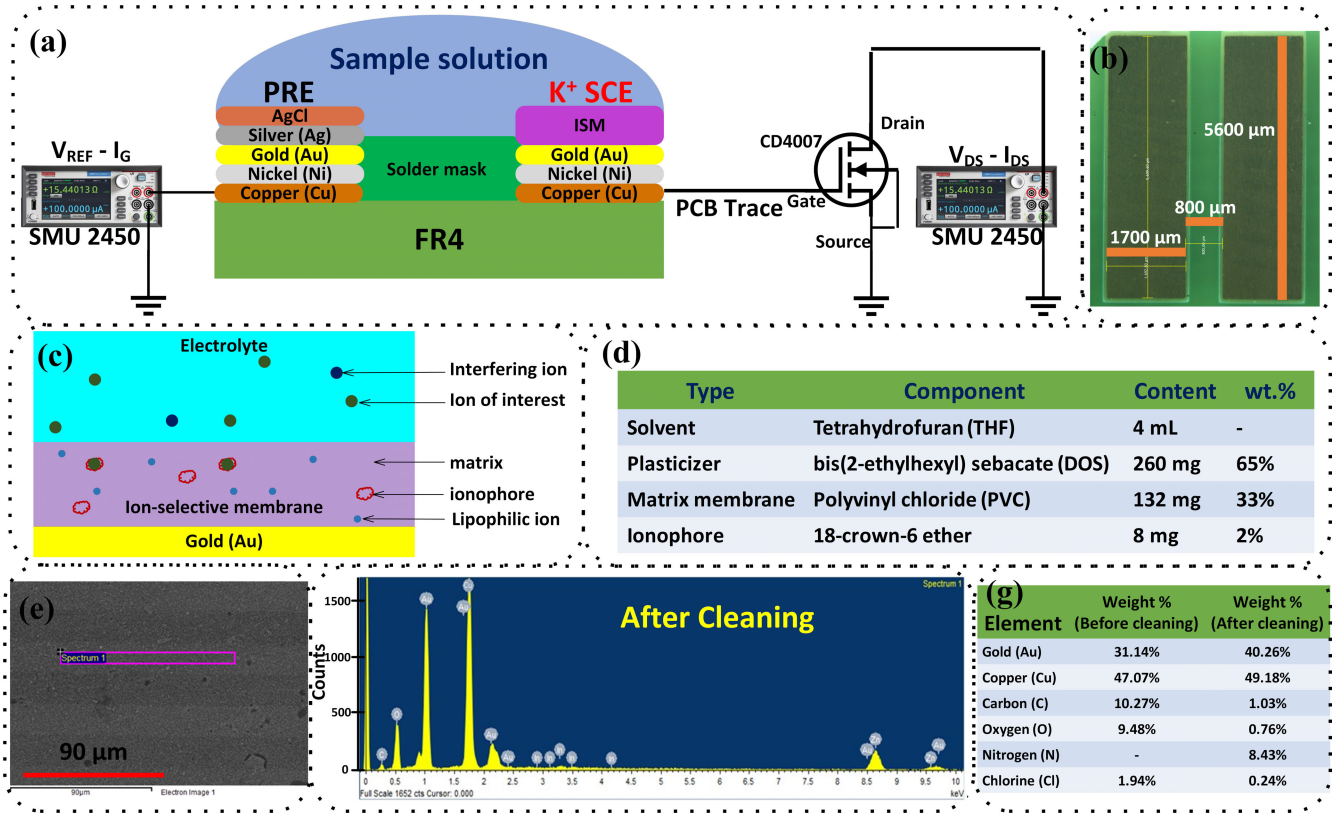

Type	Component	Content	wt.%
Solvent	Tetrahydrofuran (THF)	4 mL	-
Plasticizer	bis(2-ethylhexyl) sebacate (DOS)	260 mg	65%
Matrix membrane	Polyvinyl chloride (PVC)	132 mg	33%
Ionophore	18-crown-6 ether	8 mg	2%

Element	Weight % (Before cleaning)	Weight % (After cleaning)
Gold (Au)	31.14%	40.26%
Copper (Cu)	47.07%	49.18%
Carbon (C)	10.27%	1.03%
Oxygen (O)	9.48%	0.76%
Nitrogen (N)	-	8.43%
Chlorine (Cl)	1.94%	0.24%

FIGURE 1. (a) A circuit presentation of a platform with one sensor. The gate of the n-type MOSFET (CD4007) is connected to the sensing PAD via a copper trace. Sensing PAD (Au electrode) is coated with an ion-selective membrane (ISM), and Ag/AgCl is coated as a pseudo-reference electrode (PRE) on other gold PAD. The Voltage V_{REF} is applied to the PRE, V_{GS} is the voltage at the FET gate, and V_{DS} is the applied drain voltage. (b) top view displaying the dimensions of the ENIG Au electrode on the PCB. (c) Schematic representation of ion-selective polymeric membrane functionalization on a gold electrode (Au on PCB) (d) Cocktail compositions for ion-selective membrane (ISM) preparation (compounds were dissolved in 4.0 ml of THF solution). (e) The EDX measurement is on a section of ENIG Au coating. (f) EDX spectrum obtained from the segment shown in (e) after RCA cleaning. (g) Quantitative elemental calculation of EDX measurement before and after RCA cleaning of ENIG Au coated electrode on the PCB.

nutrient measurement. In this study, we present a low-cost and stable all-solid-state electrode on a PCB substrate for potassium sensing in an EGFET configuration for sensitivity enhancement. The Materials and Methods section describes the fabrication of all-planar ISM-coated SCE and Ag/AgCl PRE on PCB. Furthermore, we have explained the experimental setup to demonstrate the performance of (1) PRE, (2) K^+ SCE, and (3) sensitivity enhancement using EGFET. The results show that the low-cost and non-toxic K^+ EGFET exhibits high voltage sensitivity of -49 mV/log[K+], current sensitivity $(1.43(\mu A)^{1/2}/log[K+])$, a large linear range of detection (10^{-4} - 1 M), and fast response ($<$ 10 seconds). Our approach represents a valuable strategy for realizing reliable, easy fabrication, non-toxic, and low-cost ion-sensing devices.

II. EXPERIMENTAL

The sensing platform consisted of an ISM-coated solid-contact electrode (SCE) and an Ag/AgCl pseudo-reference electrode (PRE) integrated on the PCB. The electrodes were mounted alongside a discrete n-type Si-FET (CD4007, Texas Instruments) to ensure chemical isolation and electrical connectivity on a custom-printed circuit board (PCB). Fig. 1(a) shows the structural details of the ISM-coated SCE and Ag/AgCl PRE on an ENIG-Au-plated PCB in an EGFET configuration.

A. MATERIAL AND METHODS

The electrode arrays were designed using Autodesk EAGLE 9.5.1 and fabricated by a commercial PCB manufacturer (PCB Power Market India). Employing rigid FR4 substrate and 100 μm copper traces has ensured durability and stable electrical properties. The rectangular area, measuring 5.6 mm by 1.7 mm, has undergone electroless nickel immersion gold (ENIG) surface plating, providing enhanced conductivity and corrosion resistance (Fig. 1(b)). This process has yielded a two-layer metallic coating (100 nm Au over 5 μm Ni), ensuring a stable and inert surface for subsequent functionalization. The different functionalized gold electrode arrays served as sensing and reference electrodes, enabling precise electrochemical measurements. A liquid photoimageable solder mask has been applied to encapsulate traces, safeguard against electrical interference and enhance longevity while maintaining the signal integrity.

Furthermore, a 15-minute ultrasonication bath in each solvent; acetone, IPA, and water, sequentially, was required for electrode cleaning. An additional step was required to clean the gold-plated electrode before functionalization with SCE and PRE to remove organic contamination. The RCA SC-1 cleaning method involves 30-minutes of ultrasonication in a solution containing 5:1:1 water, ammonium hydroxide (20%), and hydrogen peroxide (30%). The EDX measurements have been conducted within the pink rectangular region situated at the top of the gold electrode on the PCB, as depicted in Fig. 1(e). Subsequently, Fig. 1(f) illustrates the EDX spectrum obtained post-RCA cleaning for elemental analysis. Additionally, Fig. 1(g) provides a tabulated summary of quantitative elemental calculations, showcasing the effective removal of organic contaminants. The stability of the electrical response before and after additional RCA cleaning has been demonstrated in Fig. S1 of the supplementary material.

B. PREPARATION OF SENSING AREA

Ionophores such as valinomycin [20], [34], and 18-crown-6-ether [5] have been reported in the literature for potassium sensing. Valinomycin falls into category 1 of acute toxicity, whereas 18-crown-6 ether falls into category 4 [29]. Here, we have utilized 18-crown-6 ether as a potassium ionophore since we intended to use a non-toxic sensor in an open field. Selectophore ® grade potassium ionophore (18-Crown-6 $\geq$ 99.0%), bis(2-ethylhexyl) sebacate (DOS), high molecular weight polyvinyl chloride (PVC), and anhydrous tetrahydrofuran (THF) ($\geq$ 99.0%, inhibitor-free) have been purchased from Sigma Aldrich. Crown ethers have exhibited stronger affinities, and the cation selectivity for alkali metal ions is mainly dependent on the size and charge density of the ion and cavity size of the crown ether. The working principle of the crown ether ionophore is illustrated in Fig. 1(c).

A typical cocktail solution consists of 2 wt % ionophore, 65 wt % plasticizers DOS, and 33 wt % membrane matrix PVC [23], and all components have been dissolved in THF (Fig. 1(d)). So, the potassium ISM has been prepared by dissolving 8 mg of 18-crown-6 ether with 260 mg of DOS. The separate solution of 132 mg PVC in 4 ml of THF has been prepared by ultrasonicating the mixture for half an hour. A solution has been kept overnight to ensure the dissolution of PVC. Further, both the solutions have been mixed together and briefly shaken using an ultrasonicator. Now, a volume of 4 μL ISM cocktail has been drop-casted over the gold SCE within the confined 3D-printed mould and then dried overnight.

Similarly, for the reference electrode (RE), silver conductive paste (resistivity: 0.01 to 0.05 Ω/sq) has been uniformly coated on top of non-encapsulated gold (Au). Furthermore, a small drop of sodium hypochlorite NaOCl solution (NaOCl, Sigma-Aldrich, reagent grade, available chlorine 4.00% - 4.99%) has been kept on the exposed silver. After 10 minutes, the electrode has been washed with DI water and dried using a nitrogen gun, chlorinating the top layer of silver into silver chloride (AgCl). The change in the color of the silver layer to brownish after chlorination represents the AgCl layer being formed on top of the silver layer, as shown in the inset of Fig. 2. The stability of the electrical response using the three different chlorination processes has been compared in Fig. S2 of the supplementary material.

C. ELECTROMOTIVE FORCE MEASUREMENTS (EMF)

All current-voltage measurements have been conducted under dark conditions within a Faraday cage to avoid any interference. We have utilized a cylindrical chamber made of Teflon to serve as the test cell to contain the analyte solution throughout the entire measurement process. All measurements have been conducted at room temperature (300$\pm$5 K). It is important to note that changes in solution temperature can impact sensor sensitivity, as per Nernst's law, which is directly proportional to temperature.

The sensitivity of the K^+ ISE has been determined by measuring in diluted KNO_3 solution over a concentration range from 1 M to 10^{-6} M in steps of 10^{-1} M of $[K^+]$ ion. After measuring the electrode in a solution for 600 seconds, the electrode has been immediately cleaned with DI water for 60 seconds, then quickly immersed in the next solution. The ion-sensing properties in terms of sensitivity, stability, range, linearity, hysteresis, drift, repeatability, and pH effect have been measured for all the K^+ concentrations.

D. EGFET CONFIGURATION MEASUREMENTS

The sensor's performance in the EGFET configuration has been evaluated by measuring the I-V characteristics using two Keithley 2450 Source Measure Units (SMUs). The KickStart Instrument Control Software version 2.9.0 was utilized for the synchronization and simultaneous data acquisition of the two SMUs. The performance assessment of SCE and PRE in the EGFET configuration has been conducted across various $[K^+]$ concentrations ranging from 1 to 10^{-6} M.

Transfer characteristics have been recorded by sweeping the reference voltage (V_{REF}) from 0 V to 5 V with $V_{DS} = 0.5$ V across different $[K^+]$ solutions. The output characteristics ($I_{DS} - V_{DS}$) have been recorded by sweeping V_{DS} from 0 V to 5 V while operating the off-the-shelf MOSFET (CD4007) in the saturated region at a voltage V_{REF} of 2 V. The baseline transfer and output characteristics have been measured by short-circuiting the SCE and PRE without the presence of an analyte solution. The change in threshold voltage ($\Delta V_{T(EGFET)}$) and voltage sensitivity have been calculated using the transfer characteristics, whereas enhanced current sensitivity and linearity have been determined using the output characteristics.

III. RESULTS

A. PERFORMANCE OF PSEUDO REFERENCE ELECTRODE (PRE)

The performance of the Ni/Au/Ag/AgCl structure (pseudo-RE) has been evaluated by measuring the open-circuit

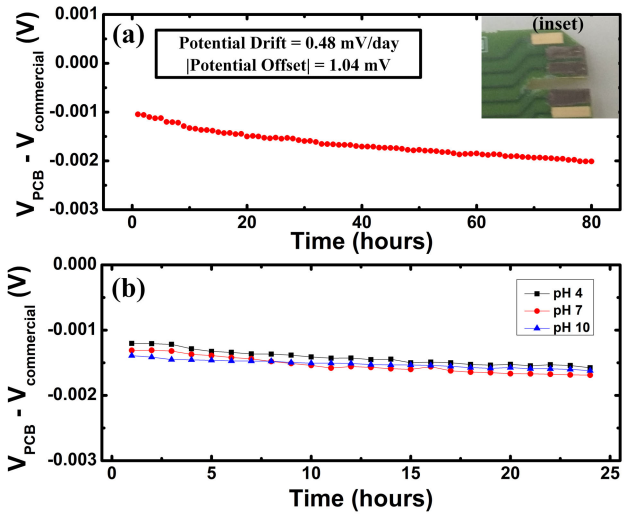

FIGURE 2. (a) Potential difference between pseudo reference electrode (PRE) on PCB and commercial Ag/AgCl reference electrode (V_{PCB} - $V_{commercial}$) evolution over 3 days at neutral pH. The chlorine ion effect and brownish color of the Ag/AgCl electrode (inset). (b) Evaluation of the effect of pH (4,7, and 10) on PRE (V_{PCB} - $V_{commercial}$) for a day.

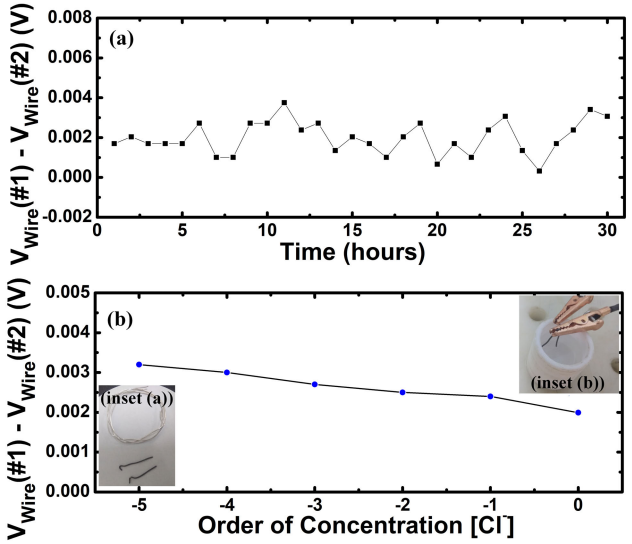

FIGURE 3. (a) Potential difference between two Ag/AgCl wire PRE evaluations for a day. (b) Potential difference between two Ag/AgCl wire PRE versus the effect of chloride ion [Cl^+] concentration. Silver (Ag) wire and two AgCl-coated PRE (inset (a)). Two PRE wires were dipped in the test solution for potential difference (V_{Wire}(#1) – V_{Wire}(#2)) measurement (inset(b)).

potential (V_{OCP}) of the PRE against the commercial glass Ag/AgCl reference electrode ($V_{PCB} - V_{commercial}$) over three days in a 3 M KCl solution, as represented in Fig. 2(a). The suitability of an electrode as a reference electrode relies on its ability to maintain a stable open-circuit potential, low offset potential and minimal drift potential. The offset potential, measured at a remarkable 1.04 mV, further underscores the electrode's exceptional performance. The PRE has also exhibited a very long-standing electrical behaviour term with the potential drift ($\Delta E/\Delta t = 0.48\, mV/day$) of less than 1 mV for 3 days. The drift in potential is attributed to the dissolution of the AgCl layer in the dipped solution [35].

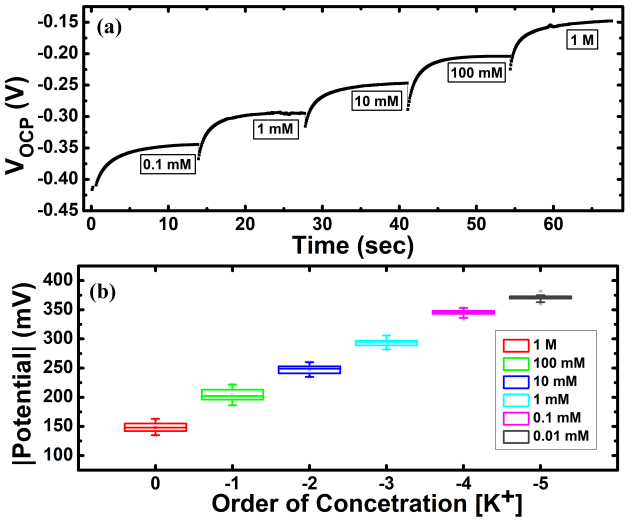

FIGURE 4. Carry-over test for various [K^+] ranging from 10^{-5} M to 1 M. (a) Transient response of potential generation (Electromotive force measurement) at different concentrations. The sensor exhibits a fast response time to changes in concentration. (b) Mean value and the standard deviation of the sensor OCP response of 24 different devices with respect to [K^+] ion concentration.

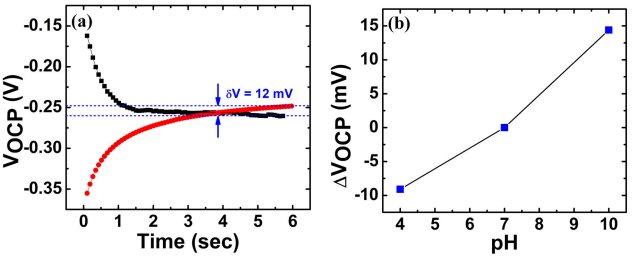

FIGURE 5. (a) Hysteresis (δV) characteristics as a factor test representing the reversibility of sensor performance. (b) Change in the open-circuit potential of the sensor w.r.t different pH.

Additionally, for all three different pH buffers (pH = 4, 7, and 10), the PRE electrodes have demonstrated long-term electrical stability (Fig. 2(b)). Furthermore, the offset potential is two mV (at max) irrespective of the buffer solution pH as compared to commercial Ag/AgCl glass electrodes. This indicates the diffusion of ions from the sample to the PRE junction has been negligible regardless of the buffer solution pH, and the junction potential has been less than five mV and reproducible.

To analyze the potential difference between the two PREs. The same chlorination process has been followed for two silver wires (Fig. 3 inset(a)), and the time evolution of the difference in OCP has been measured in 1 M KCl solution ($[Cl^-] = 10^0\, M$) (Fig. 3 inset(b)). The difference in potential has remained almost constant for the duration of 24 hours, validating the stability of the PRE (Fig. 3(a)). Furthermore, V_{OCP} for two different PRE wires has been measured across all chloride concentrations, corroborating the stable potential difference (Fig. 3(b)).

B. PERFORMANCE OF K^+ SCE

Fig. 4(a) shows the open circuit potential (OCP) between the SCE and PRE with respect to time immersed in the solution

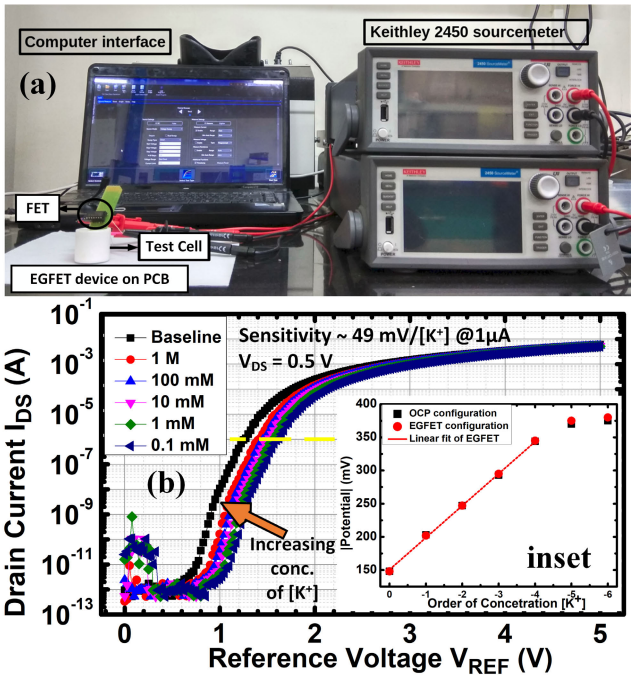

FIGURE 6. (a) Measurement set-up of an EGFET-based potentiometric sensor system. (b) Transfer characteristics ($I_{DS} - V_{REF}$) of $[K^+]$ ion-sensitive EGFET at different concentrations. (inset) V_{OCP}, $V_{T(EGFET)}$ and curve fit to demonstrate slope and linearity.

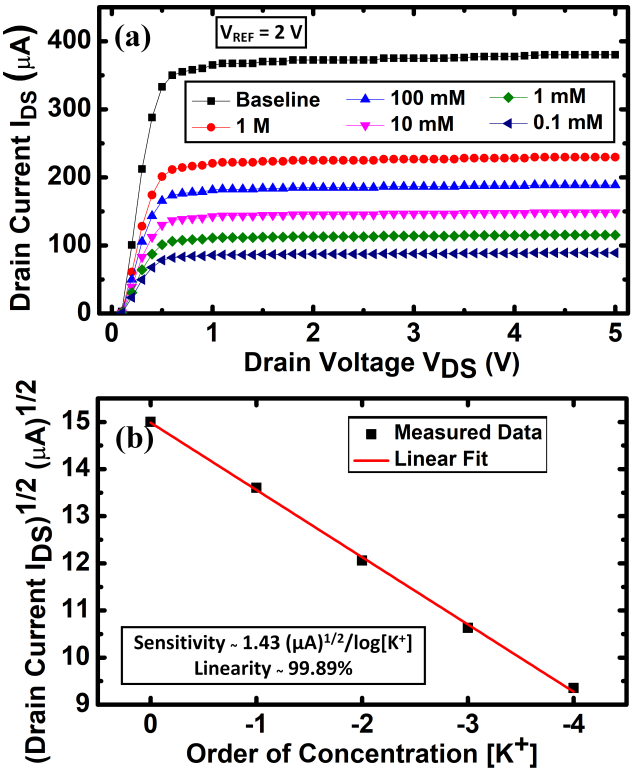

FIGURE 7. (a) Output characteristics ($I_{DS} - V_{DS}$) for the $[K^+]$ ion-sensitive EGFET are in the saturation region for different concentrations. (b) Linearity of the $(I_{DS})^{1/2}$ of sensor w.r.t. order of $[K^+]$ concentration.

with varying ionic concentrations of KNO_3. The output of the sensor has been recorded for 600 seconds in each solution. The figure also evidences that the potential stabilization has been achieved in less than 10 seconds. Furthermore, in Fig. 4(b), a calibration curve has been generated for 24 different SCEs, plotting the potential value against $[K^+]$ ion concentration. This curve illustrates the mean and range of V_{OCP} for specific $[K^+]$ ion concentrations. Our sensing device has demonstrated a standard deviation of less than 10 mV, highlighting its precision. Furthermore, the change in the mean V_{OCP} (ΔV_{OCP}) has been utilized to calculate the voltage sensitivity. The ΔV_{OCP} reveals that the SCE has demonstrated a sensitivity of $-49\ mV/decade$ in the linear range from $10^{-4}\ M$ to $1\ M$, which is ideal for soil sensing applications [36].

The V_{OCP} is the electrochemical potential difference between the SCE and PRE and can be expressed by the Nernst equation. The Nernst equation of the electrode potential for real solutions presenting ions of interest i and interfering species j is:

$$E = E^0 + \frac{RT}{z_i F} ln\left(a_i + \sum K_{ij}^{pot} (a_j)^{Z_i Z_j}\right) = V_{OCP} \qquad (1)$$

where, E is the electrode potential, E^0 is the standard electrode potential, R is the gas constant, T is the absolute temperature, z is the valence of the ion, F is the Faraday constant, K_{ij}^{pot} is the selectivity coefficient, a_i is the concentration of primary ion and a_j is the concentration of the interfering ion. Umezawa et al. have compiled the selectivity of all ISE, and the selectivity of crown ether has already been studied [37], [38].

We have also carried out a test to evaluate the hysteresis of SCE against PRE by changing the stepwise concentration from $10^{-4}\ M$ to $1\ M$ and then reversing the order. The net hysteresis has been calculated as the difference between the V_{OCP} (δV) at a particular concentration during an upward and downward shift in concentration. Fig. 5(a) represents the hysteresis of 12 mV for the $[K^+] = 10^{-2}\ M$ concentration. This result is better than the previously reported result for K^+ SCE on ENIG-Au-based PCB, which was 24.8 mV [20]. The ions in the electrolyte chemically interact with the surface defects of the membrane and/or slow-reacting sites between the electrode and the membrane, causing hysteresis [39].

Furthermore, we have established the pH invariance of the SCE (selectivity against the H^+ ion). Three pH values (4, 7, and 10) have been used to measure the open circuit potential of the constant concentration of potassium ($10^{-2}\ M$). The pH has been adjusted by the adding dilute nitric acid or sodium hydroxide, as appropriate. Fig. 5(b) shows the difference between V_{OCP} (at pH 4 and pH 10) and V_{OCP} (at pH 7). If the δV_{OCP} is within the range of 20 mV, the electrode is considered stable [40]. It has been observed that the electrode responses have been independent over a nominal soil pH range.

C. PERFORMANCE OF EGFET CONFIGURATION

Fig. 6(a) shows the measurement set-up of the all-solid-state [K+] ion sensor in the EGFET configuration. The transfer

TABLE 1. Comparative analysis of all main parameters of K+ SCE potentiometric ion sensing measurements in several recent works.

Reference	Electrode	Ionophore	Sensitivity (mV/decade)	Linear detection range (M)	Response time (sec)	Potential drift	LOD (10^{-n} M)	PRE	Cost	Toxicity
[5]	Platinum electrode	Crown ether series	-50.2 $mV/log[K^+]$	$10^{-1}-10^{-4.8}$ M	20 sec	$<$ 0.1 mV/min	$10^{-4.8}$ M	No	High	No
[41]	Glassy carbon electrode	Valinomycin	58.4 $mV/log[K^+]$	$10^{-1}-10^{-5.8}$ M	$<$ 10 sec	12.6 $\mu V/h$	$10^{-6.2}$ M	No	Very High	Yes
[34]	Inkjet printed graphene	Valinomycin	57.2 $mV/log[K^+]$	$10^{-2}-10^{-5}$ M	$<$ 10 sec	8.6 $\mu V/sec$	$10^{-5.15}$ M	No	Low	Yes
[20]	Hard Au on FR4 PCB	Valinomycin	54 $mV/log[K^+]$	$10^{-1}-10^{-4}$ M	250 sec	32.4 mV/day	10^{-5} M	Yes	High	Yes
[20]	ENIG Au on FR4 PCB	Valinomycin	22.2 $mV/log[K^+]$	$10^{-1}-10^{-4}$ M	300 sec	28.6 mV/day	10^{-5} M	Yes	Low	Yes
[42]	Glassy carbon electrode	Valinomycin	55.03 $mV/log[K^+]$	$10^{-1}-10^{-5}$ M	6-8 sec	5.17 mV/h	$10^{-5.23}$ M	No	Very High	Yes
This work	ENIG Au on FR4 PCB	Crown ether series	-49 $mv/log[K^+]$	$10^{0}-10^{-4}$ M	$<$ 10 sec	57.17 $\mu V/sec$	10^{-6} M	Yes	Low	No

characteristics ($I_{DS}-V_{REF}$) are shown in Fig. 6(b) with $V_{DS} = 0.5$ V. The $I_{DS} - V_{REF}$ curve in the linear region shows a uniform shift in the threshold voltage from left to right as the $[K^+]$ concentration decreases. In accordance with EGFET theory, $V_{T(EGFET)}$ is expressed by the following formula,

$$V_{T(EGFET)} = V_{T(MOSFET)} + \frac{\Phi_M}{q} + E_{REF} + \chi^{sol} - \varphi \quad (2)$$

where $V_{T(MOSFET)}$ is the threshold voltage of FET, Φ_M is the reference electrode gate metal work function, E_{REF} is the reference electrode potential, χ^{sol} represents the surface dipole potential of the buffer solution, and φ symbolizes the surface potential at the electrolyte/sensing film interface.

The $[K^+]$ ion sensitivity and linearity of the sensor have been derived from the transfer characteristics at $I_{DS} = 1$ μA (yellow dashed line in Fig. 6(b)) at various $[K^+]$ concentrations and are plotted in the inset of Fig 6(b). The $[K^+]$ ion voltage sensitivity and linearity are determined as follows:

$$\begin{aligned} \textit{Voltage sensitivity} &= \frac{V_{T(EGFET)}(x1) - V_{T(EGFET)}(x2)}{log[K^+](x1) - log[K^+](x2)} \\ &= \frac{\Delta V_{T(EGFET)}}{\Delta log[K^+]} \end{aligned} \quad (3)$$

The sensitivity of the sensor has been calculated to be -49.11 mV/log$[K^+]$ with a standard deviation of 8.74 mV, and the linearity has been revealed to be 99.81%. Considering an error of 1 K leads to 0.2 mV/log$[K^+]$, resulting in a variation of $\pm$ 1 mV/log$[K^+]$ in the sensor output at room temperature (300 $\pm$ 5 K). Therefore, the temperature effect on the sensor output was within the experimental error and was negligible.

The modification of $V_{T(EGFET)}$ in the potentiometric electrochemical sensor in the EGFET configuration correlates simply with the change in electrochemical potential, as expressed by $\Delta V_{OCP} = -\Delta V_{T(EGFET)}$.

Furthermore, Fig. 7(a) has demonstrated the output characteristics ($I_{DS} - V_{DS}$) of the $[K^+]$ ion sensor when the MOSFET has been operating in the saturation region at V_{REF} of 2 V. As the $[K^+]$ ion concentration decreased, the $I_{DS}-V_{DS}$ curve shifted downward. For the saturation region of EGFET, the $I_{DS} - V_{DS}$ can be expressed as,

$$I_{DS} = \frac{W\mu_n C_{ox}}{2L}[(V_{REF} - V_{T(EGFET)})^2]$$

where μ_0 denotes the carrier mobility, C_{ox} symbolizes the gate capacitance per unit area and W/L represents the width-to-length ratio of the channel of n-FET of CD4007. The square root of I_{DS} is the function of V_{REF}, and the $I_{DS} - V_{DS}$ can be expressed as:

$$\sqrt{I_{DS}} = \sqrt{\frac{\mu_0 C_{ox}}{2} \times \frac{W}{L}}(V_{REF} - V_{T(EGFET)})$$

The square root of I_{DS} function is the potassium ion current sensitivity in the saturation region, which is measured as $(\mu A)^{1/2}/log[K^+]$ and calculated at $V_{DS} = 2$ V. Thus the $[K^+]$ ion current sensitivity can be expressed as follows,

$$\begin{aligned} \textit{Current sensitivity} &= \frac{\sqrt{I_{DS}}(y1) - \sqrt{I_{DS}}(y2)}{log[K^+](y1) - log[K^+](y2)} \\ &= \frac{\Delta\sqrt{I_{DS}}}{\Delta log[K^+]} \end{aligned} \quad (4)$$

The calculated $[K^+]$ ion current sensitivity has been approximately 1.43 $(\mu A)^{1/2}/log[K^+]$, which is notably high, with a linearity of 99.89 % as shown in Fig. 7(b). This result indicates that $\sqrt{I_{DS}}$ linearly depends on the $[K^+]$ ion concentration in the saturation region.

IV. DISCUSSION

In this section, we have discussed the performance of our potassium-sensing EGFET compared to state-of-the-art methods, highlighting its sensitivity, detection range, precision, reliability, response time, cost, and suitability for field applications.

The sensitivity magnitude of potentiometric measurement for potassium sensing, at 49 mV/log$[K^+]$, typically falls within the lower end of the state-of-the-art sensitivity range reported in other studies, which typically ranges between 50 and 60 mV/log$[K^+]$ (Table1). However, compared to previous literature on potassium sensing using ISM-coated on

ENIG Au electrode on PCB, it represents a vast improvement from 22.2 mV/log[K^+] [20]. The low sensitivity is attributed to the use of crown ether as the ion-selective membrane (ISM) instead of valinomycin employed by other researchers. Moreover, crown ether ensures that our sensor is non-toxic, making it environmentally friendly and suitable for field applications. This feature has been particularly advantageous, allowing for the safe handling and disposal of the sensor while minimizing potential environmental harm.

We have compensated for this low potentiometric sensitivity by enhancing it using an off-the-shelf FET. We have achieved 1.43 $(\mu A)^{1/2}/log[K^+]$ of $[K^+]$ ion current sensitivity. Kabba et al., 2019 have achieved 1.04 $(\mu A)^{1/2}/log[K^+]$ [32], whereas Ashoka et al., 2022 have achieved 0.73 $(\mu A)^{1/2}/log[K^+]$ as $[K^+]$ ion EGFET sensitivity [31]. Furthermore, the soil potassium concentration ranged from 10^{-2} to 10^{-4} M [36]; hence, our device's detection range is highly applicable to soil sensing. Moreover, our device's limit of detection (LOD) is impressively low. Our device has been capable of detecting potassium ions at concentrations as low as 10^{-6} M, surpassing the LOD reported in previous literature featuring valinomycin as the ISM.

Our K^+ SCE has exhibited remarkable stability, maintaining a stable V_{OCP} for 2 days in 1 M K^+ solution with a drift potential of 57.7 $\mu V/sec$, aligning closely with state-of-the-art technology. It has demonstrated a hysteresis of only 12 mV, surpassing the previous ENIG Au coating-based SCEs. The K^+ SCE has also maintained consistent V_{OCP} across a pH range of 4 to 10, enhancing its versatility. Similarly, the PRE has displayed a minimal potential drift $(\Delta E/\Delta t)$ of less than 1 mV over three days and has been pH-insensitive within the range of 4 to 10, making it suitable for diverse soil conditions. These stable characteristics have made our sensor structure reliable and valuable for agricultural and environmental monitoring applications.

Another significant advantage of our device has been its fast response time. Our device has exhibited a response time of less than 10 seconds, considerably faster than what has been reported in the existing literature. This rapid response has been highly desirable for point-of-care (POC) technology, where real-time measurements have been required for on-site decision-making. Our device has also offered another significant benefit: pH invariance, maintaining its open-circuit potential and sensitivity throughout a pH range of 4 to 10. The soil pH typically ranges between 5.5 and 8.0, though it can change based on the geographical area and the crops grown there.

V. CONCLUSION

In conclusion, we have successfully developed a non-toxic and low-cost potassium ion sensor using an extended gate field-effect transistor (EGFET) configuration with all-solid-state electrodes on a printed circuit board (PCB) substrate. A pseudo-reference electrode (PRE) based on Ag/AgCl has demonstrated excellent stability and reproducibility. The ion-selective membrane (ISM) coated on the ENIG gold electrode has exhibited a high sensitivity of 49 mV/log[K^+], a significant linear detection range from 10^{-4} M to 1 M, and a fast response time of less than 10 seconds. The sensor has displayed negligible hysteresis and remained stable over a wide range of pH values. The EGFET-based potentiometric sensing system has shown a high current sensitivity of 1.43 $(\mu A)^{1/2}/log[K^+]$. Our approach presents a practical and reliable solution for soil nutrient measurements in precision agriculture, offering significant advantages over existing potassium sensors in terms of cost, sensitivity, stability, and toxicity concerns associated with traditional ionophores. This novel sensor holds promise for optimizing agricultural output and reducing environmental impact through efficient nutrient monitoring and intelligent irrigation and fertilization management systems.

REFERENCES

[1] D. Kim, A. Kadam, S. Shinde, R. G. Saratale, J. Patra, and G. Ghodake, "Recent developments in nanotechnology transforming the agricultural sector: A transition replete with opportunities," *J. Sci. Food Agricult.*, vol. 98, no. 3, pp. 849–864, Nov. 2017.

[2] Y. Shao and Y. He, "Nitrogen, phosphorus, and potassium prediction in soils, using infrared spectroscopy," *Soil Res.*, vol. 49, no. 2, p. 166, 2011.

[3] G. Hu, K. A. Sudduth, D. He, D. B. Myers, and M. V. Nathan, "Soil phosphorus and potassium estimation by reflectance spectroscopy," *Trans. ASABE*, vol. 59, no. 1, pp. 97–105, 2016.

[4] B. Kashyap and R. Kumar, "Sensing methodologies in agriculture for soil moisture and nutrient monitoring," *IEEE Access*, vol. 9, pp. 14095–14121, 2021.

[5] W.-S. Han, Y.-H. Lee, K.-J. Jung, S.-Y. Ly, T.-K. Hong, and M.-H. Kim, "Potassium ion-selective polyaniline solid-contact electrodes based on 4',4"(5")-di-tert-butyldibenzo-18-crown-6-ether ionophore," *J. Anal. Chem.*, vol. 63, no. 10, pp. 987–993, Oct. 2008.

[6] H.-J. Kim, K. A. Sudduth, and J. W. Hummel, "Soil macronutrient sensing for precision agriculture," *J. Environ. Monitor.*, vol. 11, no. 10, p. 1810, 2009.

[7] U. Lehmann and A. Grisel, "Miniature multisensor probe for soil nutrient monitoring," *Proc. Eng.*, vol. 87, pp. 1429–1432, Jan. 2014.

[8] M. Kaisti, "Detection principles of biological and chemical FET sensors," *Biosensors Bioelectron.*, vol. 98, pp. 437–448, Dec. 2017.

[9] J. Artigas, A. Beltran, C. Jimenez, A. Baldi, R. Mas, C. Dominguez, and J. Alonso, "Application of ion sensitive field effect transistor based sensors to soil analysis," *Comput. Electron. Agricult.*, vol. 31, no. 3, pp. 281–293, May 2001.

[10] Y. Miyahara and W. Simon, "Comparative studies between ion-selective field effect transistors and ion-selective electrodes with polymeric membranes," *Electroanalysis*, vol. 3, nos. 4–5, pp. 287–292, May 1991.

[11] I. Gracia, C. Cané, M. Lozano, and J. Esteve, "On-line determination of the degradation of ISFET chemical sensors," *Sens. Actuators B, Chem.*, vol. 15, nos. 1–3, pp. 218–222, Aug. 1993.

[12] J. Van Der Spiegel, I. Lauks, P. Chan, and D. Babic, "The extended gate chemically sensitive field effect transistor as multi-species microprobe," *Sens. Actuators*, vol. 4, pp. 291–298, Jan. 1983.

[13] P. D. Batista and M. Mulato, "ZnO extended-gate field-effect transistors as pH sensors," *Appl. Phys. Lett.*, vol. 87, no. 14, Sep. 2005, Art. no. 143508.

[14] C. M. Yang, J. C. Wang, T. W. Chiang, Y. T. Lin, T. W. Juan, T. G. Chen, M. Y. Shih, C. E. Lue, and C. S. Lai, "Hydrogen ion sensing characteristics of IGZO/Si electrode in EGFET," *Int. J. Nanotechnol.*, vol. 11, no. 1, p. 15, 2014.

[15] E. M. Guerra, G. R. Silva, and M. Mulato, "Extended gate field effect transistor using V2O5 xerogel sensing membrane by sol–gel method," *Solid State Sci.*, vol. 11, no. 2, pp. 456–460, Feb. 2009.

[16] A. Bozkurt, R. F. Gilmour, and A. Lal, "In vivo electrochemical characterization of a tissue–electrode interface during metamorphic growth," *IEEE Trans. Biomed. Eng.*, vol. 58, no. 8, pp. 2401–2406, Aug. 2011.

[17] T. Prodromakis, Y. Liu, J. Yang, D. Hollinghurst, and C. Toumazou, "A novel design approach for developing chemical sensing platforms using inexpensive technologies," in *Proc. IEEE Biomed. Circuits Syst. Conf. (BioCAS)*, Nov. 2011, pp. 369–372.

[18] T. Trantidou, D. J. Payne, V. Tsiligkiridis, Y.-C. Chang, C. Toumazou, and T. Prodromakis, "The dual role of parylene C in chemical sensing: Acting as an encapsulant and as a sensing membrane for pH monitoring applications," *Sens. Actuators B, Chem.*, vol. 186, pp. 1–8, Sep. 2013.

[19] D. Moschou, T. Trantidou, A. Regoutz, D. Carta, H. Morgan, and T. Prodromakis, "Surface and electrical characterization of Ag/AgCl pseudo-reference electrodes manufactured with commercially available PCB technologies," *Sensors*, vol. 15, no. 8, pp. 18102–18113, Jul. 2015.

[20] S. Anastasova, P. Kassanos, and G.-Z. Yang, "Multi-parametric rigid and flexible, low-cost, disposable sensing platforms for biomedical applications," *Biosensors Bioelectron.*, vol. 102, pp. 668–675, Apr. 2018.

[21] W.-J. Lan, X. U. Zou, M. M. Hamedi, J. Hu, C. Parolo, E. J. Maxwell, P. Bühlmann, and G. M. Whitesides, "Paper-based potentiometric ion sensing," *Anal. Chem.*, vol. 86, no. 19, pp. 9548–9553, Sep. 2014.

[22] J. R. Zhang, M. Rupakula, F. Bellando, E. G. Cordero, J. Longo, F. Wildhaber, G. Herment, H. Guerin, and A. M. Ionescu, "All CMOS integrated 3D-extended metal gate ISFETs for pH and multi-ion (Na^+, K^+, Ca^{2+}) sensing," in *IEDM Tech. Dig.*, Dec. 2018, p. 12.

[23] P. Bühlmann, E. Pretsch, and E. Bakker, "Carrier-based ion-selective electrodes and bulk optodes. 2. Ionophores for potentiometric and optical sensors," *Chem. Rev.*, vol. 98, no. 4, pp. 1593–1688, Jun. 1998.

[24] T. N. T. Tran, S. Qiu, and H.-J. Chung, "Potassium ion selective electrode using polyaniline and matrix-supported ion-selective PVC membrane," *IEEE Sensors J.*, vol. 18, no. 22, pp. 9081–9087, Nov. 2018.

[25] R. P. Daniele and S. K. Holian, "A potassium ionophore (valinomycin) inhibits lymphocyte proliferation by its effects on the cell membrane," *Proc. Nat. Acad. Sci. USA*, vol. 73, no. 10, pp. 3599–3602, Oct. 1976.

[26] D. Hoornstra, M. A. Andersson, R. Mikkola, and M. S. Salkinoja-Salonen, "A new method for in vitro detection of microbially produced mitochondrial toxins," *Toxicol. Vitro*, vol. 17, nos. 5–6, pp. 745–751, Oct. 2003.

[27] V. V. Teplova, R. Mikkola, A. A. Tonshin, N.-E.-L. Saris, and M. S. Salkinoja-Salonen, "The higher toxicity of cereulide relative to valinomycin is due to its higher affinity for potassium at physiological plasma concentration," *Toxicol. Appl. Pharmacol.*, vol. 210, nos. 1–2, pp. 39–46, Jan. 2006.

[28] V. Teplova, E. Jääskeläinen, M. Salkinoja-Salonen,N.-E.-L. Saris, M. Serlachius, F.-Y. Li, and L. C. Andersson, "Differentiated Paju cells have increased resistance to toxic effects of potassium ionophores," *Acta Biochimica Polonica*, vol. 51, no. 2, pp. 539–544, Jun. 2004.

[29] *Pubchem Compound Lcss for CID 441139*, Cyclo, Jul. 2023.

[30] R. Cánovas, S. P. Sánchez, M. Parrilla, M. Cuartero, and G. A. Crespo, "Cytotoxicity study of ionophore-based membranes: Toward on-body and in vivo ion sensing," *ACS Sensors*, vol. 4, no. 9, pp. 2524–2535, Aug. 2019.

[31] S. A. Asoka, L. H. Slewa, and T. A. Abbas, "Multi-ion (Na^+/K^+/Ca^{2+}/Mg^{2+}) EGFET sensor based on heterostructure of ZrO_2-NPs/MacroPSi," *Chem. Papers*, vol. 77, no. 3, pp. 1351–1360, Mar. 2023.

[32] E. A. Kabaa, S. A. Abdulateef, N. M. Ahmed, Z. Hassan, and F. A. Sabah, "A novel porous silicon multi-ions selective electrode based extended gate field effect transistor for sodium, potassium, calcium, and magnesium sensor," *Appl. Phys. A, Solids Surf.*, vol. 125, no. 11, p. 753, Oct. 2019.

[33] Q. Li, W. Tang, Y. Su, Y. Huang, S. Peng, B. Zhuo, S. Qiu, L. Ding, Y. Li, and X. Guo, "Stable thin-film reference electrode on plastic substrate for all-solid-state ion-sensitive field-effect transistor sensing system," *IEEE Electron Device Lett.*, vol. 38, no. 10, pp. 1469–1472, Oct. 2017.

[34] Q. He, S. R. Das, N. T. Garland, D. Jing, J. A. Hondred, A. A. Cargill, S. Ding, C. Karunakaran, and J. C. Claussen, "Enabling inkjet printed graphene for ion selective electrodes with postprint thermal annealing," *ACS Appl. Mater. Interfaces*, vol. 9, no. 14, pp. 12719–12727, Mar. 2017.

[35] Z. Zhang, J. Hu, Y. Ma, Y. Wang, H. Huang, Z. Zhang, J. Wei, S. Yin, and Q. Yu, "A state-of-the-art review on Ag/AgCl ion-selective electrode used for non-destructive chloride detection in concrete," *Compos. B, Eng.*, vol. 200, Nov. 2020, Art. no. 108289.

[36] R. F. Reitemeier, "Soil potassium," *Adv. Agronomy*, vol. 3, pp. 113–164, Jan. 1951.

[37] Y. Umezawa, P. Bühlmann, K. Umezawa, K. Tohda, and S. Amemiya, "Potentiometric selectivity coefficients of ion-selective electrodes. Part I. Inorganic cations (technical report)," *Pure Appl. Chem.*, vol. 72, no. 10, pp. 1851–2082, Jan. 2000.

[38] G. G. Cross, T. M. Fyles, and V. V. Suresh, "Coated-wire electrodes containing polymer immobilized ionophores blended with poly(vinyl chloride)," *Talanta*, vol. 41, no. 9, pp. 1589–1596, Sep. 1994.

[39] A. Das, D. H. Ko, C.-H. Chen, L.-B. Chang, C.-S. Lai, F.-C. Chu, L. Chow, and R.-M. Lin, "Highly sensitive palladium oxide thin film extended gate FETs as pH sensor," *Sens. Actuators B, Chem.*, vol. 205, pp. 199–205, Dec. 2014.

[40] S. Mittal, A. Kumar, S. Kaur, and S. Kumar, "Potentiometric performance of 2-aminothiophenol based dipodal ionophore as a silver sensing material," *Sens. Actuators B, Chem.*, vol. 121, no. 2, pp. 386–395, Feb. 2007.

[41] J. Ping, Y. Wang, J. Wu, and Y. Ying, "Development of an all-solid-state potassium ion-selective electrode using graphene as the solid-contact transducer," *Electrochem. Commun.*, vol. 13, no. 12, pp. 1529–1532, Dec. 2011.

[42] K. Pietrzak, N. Krstulović, D. Blažeka, J. Car, S. Malinowski, and C. Wardak, "Metal oxide nanoparticles as solid contact in ion-selective electrodes sensitive to potassium ions," *Talanta*, vol. 243, Jun. 2022, Art. no. 123335.

VISHNURAM ABHINAV (Graduate Student Member, IEEE) was born in Patna, Bihar, India, in 1992. He received the B.Tech. degree in electrical and electronics engineering from NIT Calicut, in 2013, and the M.Tech. degree in electronics engineering with a specialization in VLSI from IIT Guwahati, in 2015. He is currently pursuing the Ph.D. degree in electrical engineering with Indian Institute of Technology Bombay (IIT Bombay). TCAD modeling of FET and bacteria modeling in biophysics. He has extensively worked in the area of device-circuit co-design and design of ESD protection devices. His current research interest includes bio/chemical sensing devices. He was a recipient of the MHRD Scholarship and the Commonwealth Scholarship.

TEJAS R. NAIK received the Ph.D. degree from Indian Institute of Technology Bombay (IIT Bombay), in 2019. He is currently a UKRI Research Fellow with the Quantum Technology Hub, James Watt School of Engineering, University of Glasgow. His current research interests include photonic integrated circuits, atomic clocks, Cu/low-k interconnects, FinFET doping, self-assembly in nanoelectronics, work function engineering, sensors, nanoelectromechanical systems, and 2-D material electronics. He was a recipient of the Padma Jyothi Gold Medal Award for research by AIARA, New Delhi.